ANNUAL PERFORMANCE MODEL OF CONCENTRATING COMPOUND PARABOLIC COLLECTOR INTEGRATED PHOTOVOLTAICS

Sneha Sriwastava
University of Massachusetts Lowell
601 Windsor Ridge Drive
Westborough, MA 01581
sneha.sriwastava@gmail.com

John Duffy
University of Massachusetts
Solar Engineering Program, One University Ave.
Lowell, MA 01854
John_Duffy@uml.edu

ABSTRACT

Concentrating Photovoltaics (CPV) with a compound parabolic concentrator use less PV material and yet provide a reasonably high power output. For this reason they are cost effective, require lower capital investment, and have the potential for large scale solar power generation. For this paper, we studied CPV using a truncated Compound Parabolic Concentrator (CPC). The aim of this paper was to develop an analytical methodology to estimate the annual power output of a stationary CPV and to assess its performance. Different orientations of the CPV were considered and their impact on the annual performance of the CPV was studied. The CPV performance was compared with that of a flat plate module (FPM). Experimental verification of the methodology was done with a prototype cell having a theoretical concentration of 2.9.

1. INTRODUCTION

The increasing cost of silicon and other photovoltaic (PV) materials has been driving up the cost of manufacturing a photovoltaic module. Alternatives to conventional FPM are being sought as there is a demand for ways to reduce the price of the module and make it more competitive. CPV promises to be an efficient alternative to an FPM, at a lower price. A truncated CPC is employed in the CPV to focus the sun into a narrow strip of PV material, thus effecting a reduction in the use of expensive photovoltaic material and lowering the cost of the entire module significantly.

However, their economic advantage is offset by the smaller window of power production. The CPV cannot harvest all the incident radiation available. There is a window of acceptable incident radiation, whose limits are defined by the acceptance angle of the CPC.

Each CPC has a fixed acceptance angle for a particular concentration ratio (CR). At a higher CR, the acceptance angle is lower and thus the CPV will receive sunlight for lesser amount of time. If the profile angle of the beam incident solar radiation is less than the acceptance angle of the CPV, then it is received inside the CPV. As the sun moves across the sky during the day, the solar profile angle varies, and with it the solar beam irradiation received inside the CPV also varies. Although, the scattered diffuse and reflected components of solar irradiation enter the CPV irrespective of the solar profile angle, the acceptance angle of the CPV controls their entry inside the CPV. Therefore, it is critical to orient the CPV suitably with respect to its acceptance angle, in order to maximize its performance.

2. METHODOLOGY

2.1. Orientation

The orientation of the CPV with respect to alignment of the CPC makes a difference to the amount of radiation it receives. The profile angle is different for each orientation. We considered two orientations in which it may be aligned. They shall be called Orientation-1 and Orientation-2, and are shown in Fig 1.

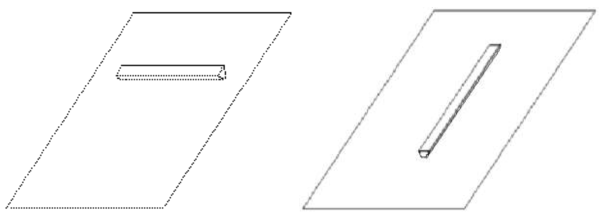

Fig. 1: Orientation-1(left); Orientation-2 (right)

2.1.1 Orientation-1

First we consider the CPV aligned parallel to the length of the CPC (i.e., east-west). Here, east-west is a notation we have used to indicate the alignment of the CPC with respect to the CPV module. Fig 2 shows the orientation relative to a simulated sloped roof. In this scenario, the profile angle of the incident solar beam normal radiation is given by a familiar equation, similar to the profile angle for an FPM:

$$\theta p1 = tan^{-1}\left(\frac{tan(90 - z)}{cos(|a_w - a_s|)}\right)$$

Fig. 2: Experimental setup (top); Close up of the cell in Orientation-1 (bottom)

However, in order to find out if the sunlight enters the CPV at any given hour, we employ a trigonometric relation between the profile angle, slope of the CPV and the acceptance angle. For the solar profile angle satisfying this relation, the beam radiation enters the CPV, in all other cases, the beam radiation does not enter the CPV. This relation is valid as long as the solar altitude angle is positive, or when the sun is above the horizon and the module.

$$\alpha > 0$$

$$\left(90 - \beta - \frac{aa_{cpc}}{2}\right) < \theta p1 < \left(90 - \beta + \frac{aa_{cpc}}{2}\right)$$

Where, the acceptance angle $\mathrm{aa_{cpc}}$ is given by the formula:

$$\mathrm{aa_{cpc}} = \sin^{-1}\left(\frac{1}{\mathrm{CR}}\right)$$

We assume that the aforementioned conditions have to be satisfied each hour of the day for the CPV to receive incident radiation. Conversely, the number of hours the equation is satisfied, that many hours of beam normal radiation enter the CPV. In other words, we ignore the irradiation that may enter from the sides of the CPC which is assumed to be made of plastic or glass.

The collector azimuth a_w is left as a variable in the derivation of the equations to allow for different roof orientations even though we call our orientations of the CPC east-west and north-south for convenience in labeling purposes.

2.1.2 Orientation-2

Secondly, the CPV could be aligned normal to the length of the CPC (i.e., north-south). In this case, the profile angle of the solar radiation has to be derived using a three dimensional model. We used vector geometry to arrive at a formula to compute this angle. Fig 3 and 4 show the relationship between the various vectors that are in the plane of the CPV and are used to calculate the profile angle. The unit vectors i, j, and k define the local coordinate system and are pointing to the south, east, and vertical (a “flag pole” normal to the horizontal plane).

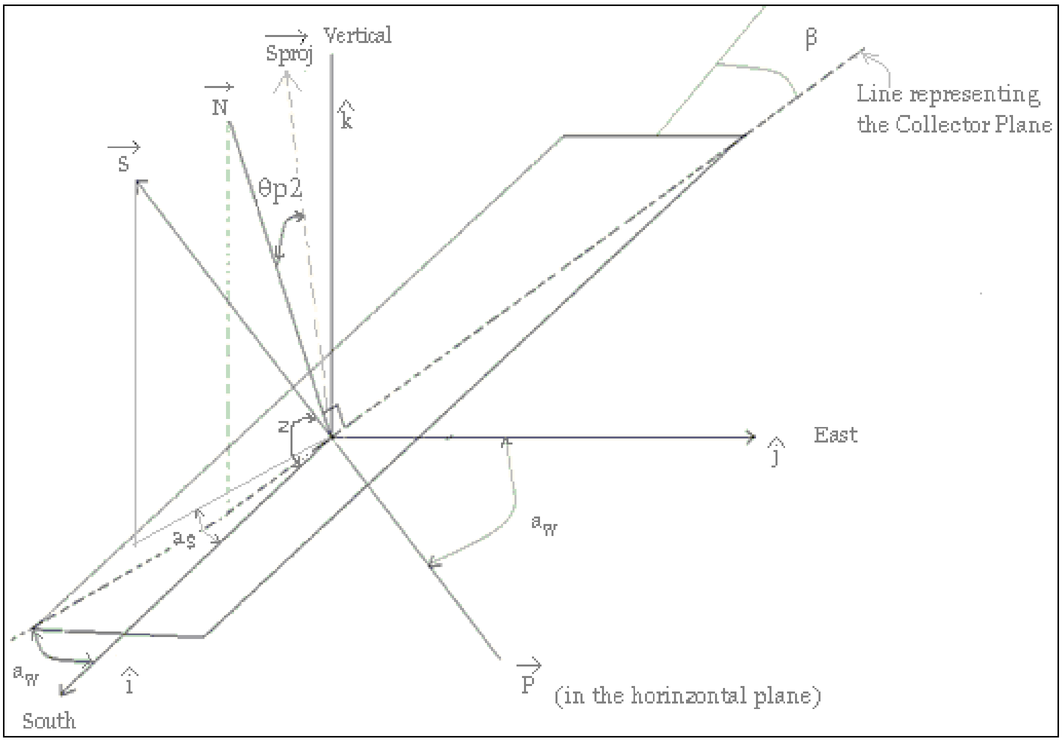

Fig. 3: The Vector Diagram of Orientation-2

$$\vec{P} = \hat{\imath}\sin a_w + \hat{\jmath}\cos a_w$$

Note that even though P is in the horizontal plane, it is also in the plane of the base of the CPC and the PV.

$$\vec{N} = \hat{\imath}\cos a_w \sin\beta + \hat{\jmath}\sin\beta\,\mathrm{sin} a_w + \hat{k}\cos\beta$$

$$\vec{S} = \hat{\imath}\cos a_s\,\mathrm{sin}z + \hat{\jmath}\sin a_s\,\mathrm{sin}z + \hat{k}\mathrm{cos}z$$

$$\vec{S}.\vec{N} = \cos i$$

$$\vec{S}.\vec{P} = \cos i_N$$

$$\vec{S}.\vec{N} = \left(\sqrt{\cos^2 a_s \sin^2 z + \sin^2 a_s \sin^2 z + \cos^2 z}\right). \left(\sqrt{\cos^2 a_w \sin^2\beta + \sin^2 a_w \sin^2\beta + \cos^2\beta}\right).\cos i$$

$$\vec{S}.\vec{N} = \left(\sqrt{\sin^2 z(\cos^2 a_s + \sin^2 a_s) + \cos^2 z}\right). \left(\sqrt{\sin^2\beta(\sin^2 a_w + \cos^2 a_w) + \cos^2\beta}\right).\cos i$$

$$\vec{S}.\vec{N} = \sqrt{\sin^2 z(1) + \cos^2 z}.\sqrt{\sin^2\beta(1) + \cos^2\beta}.\cos i = \cos i$$

$$\vec{S}.\vec{P} = \left(\sqrt{\cos^2 a_s \sin^2 z + \sin^2 a_s\ \sin^2 z + \cos^2 z}\right). \left(\sqrt{\sin^2 a_w + \cos^2 a_w}\right).\cos i_N$$

$$\vec{S}.\vec{P} = \sqrt{\sin^2 z.(\cos^2 a_s\ + \sin^2 a_s\ ) + \cos^2 z}.\sqrt{1}.\cos i_N$$

$$\vec{S}.\vec{P} = \sqrt{\sin^2 z + \cos^2 z}.\sqrt{1}.\cos i_N = \sqrt{1}.\sqrt{1}.\mathrm{cos} i_N$$

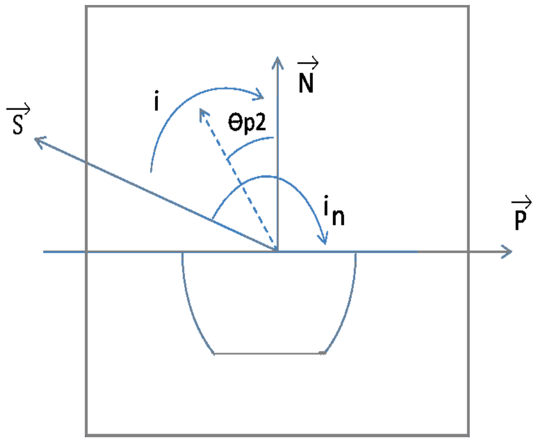

Fig. 4: The profile view of the CPV in Orientation-2 along "North-South"

$$\vec{S}.\vec{P} = 1.\cos i_N$$

$$\tan\theta p2 = \frac{\vec{S}.\vec{N}}{\vec{S}.\vec{P}} = \frac{\cos i}{\cos i_N}$$

Hence,

$$\theta p2 = \tan^{-1}\left(\frac{\cos i}{\cos i_N}\right)$$

Also, from the dot product of $\vec{S}$ and $\vec{P}$, we obtain the incident angle on that plane to be,

$$\cos i_N = \cos a_s \sin z \sin a_w + \cos a_w \sin a_s \sin z$$

In order to evaluate the sunlight hours received by the CPV, the profile angle θp2 is compared with the acceptance angle for each hour of the day. If the profile angle is less than the acceptance angle, the beam radiation enters the CPV, else it does not.

2.2 Diffuse Radiation

For a low concentrating and stationary CPV, there is some amount of scattered diffuse radiation which manages to reach inside it and hit the PV at the bottom. In this study, we quantified it to be a fraction of the global diffuse radiation and the ground reflected component of the beam normal radiation. This fraction is a function of the acceptance angle of the CPC and the collector slope. We estimated it to be -

$$\text{fraction} = \frac{2 * aa_{cpc}}{\pi - \beta}$$

This is geometrically valid for slopes less than 90 degrees, which seems reasonable.

2.3 Irradiation Calculation

As the number of sun hours harvested by the CPV and the fraction of diffuse radiation entering inside it is calculated from the above calculations, we then proceed to estimate the effective energy received by the CPV. The formulae for the calculation of the hourly irradiation entering a collector are used to calculate the amount of energy incident on the CPV,

$$I_{cpv} = I_{beam} + [\overline{R_d} \cdot I_D + \overline{R_r} \cdot I_{beam}] \cdot \text{fraction}$$

Where, the coefficients $\overline{R_d}$ and $\overline{R_r}$ are given by,

$$\overline{R_d} = \left(\frac{1 + \cos\beta}{2}\right)$$

$$\overline{R_r} = \rho_g . \left(\frac{1 - \cos\beta}{2}\right)$$

2.4 Electrical Energy Output:

Once the incident energy entering the CPV is estimated, the next step is to evaluate how much power it produces. In this study we used a simplified transmittance value of the lens for our calculations. An important factor to consider is the temperature, as the CPC gets heated quickly, due to which there can be significant temperature increase of the CPV contributing towards lower power output. Thereby, the temperature losses need to be accounted for and included in the power output calculation. The electrical energy produced also depends upon the efficiency of the CPV. This was found out by conducting some tests on the cell. Hence, the calculation of the electrical energy produced is as follows:

$$P = I_{cpv} \cdot A_{lens} \cdot \eta \cdot \tau \cdot (1 + \Delta P)$$

Where,

$$\Delta P = \Delta Tc \cdot \Delta P\%$$

Electric output of the cell is thus calibrated and then compared with the experimental results.

3. EXPERIMENTAL VERIFICATION

The model was tested by performing experiments on the prototype cell. The tests were conducted under a solar lamp

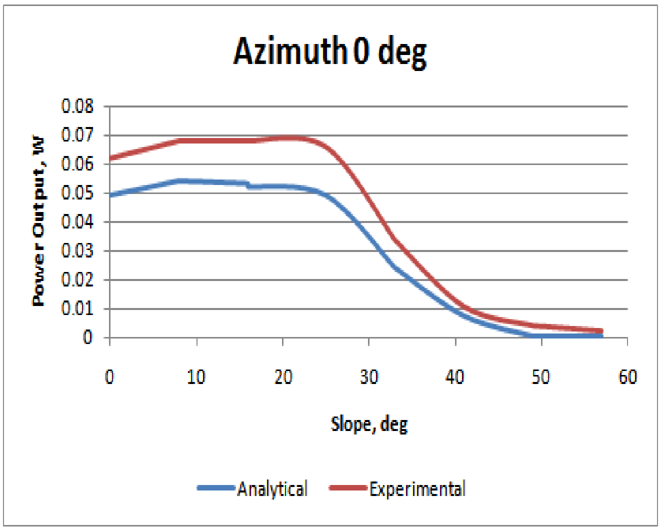

Fig. 5: Comparison of Experimental Results with Analytical Results at different slopes at 0^o azimuth

and the cell was mounted on the apparatus shown in Fig 1. First, the azimuth was fixed at zero degrees and the slope was changed to see the performance of the cell in orientation 1, Fig 5 shows the results. Next, the slope was changed at few different azimuths to see the performance of the cell in orientation 1. Fig 6 shows the results.

4. DISCUSSION

The experiments showed slightly higher energy output compared with the theoretical calculation, and the difference gets wider at higher collector slopes (although in Fig 6 due to very low values of power output at higher slopes, it appears as though the difference is greater at lower slopes, but this is not the case). This deviation can be attributed to a few factors, one of them, discretization uncertainity, due to the very small current output from the experimental module. Morover, at higher collector slopes where the profile angle is outside of the acceptance range, the current produced is extremely small resulting in higher discretization uncertainty. Finally, the model is more conservative due to the fact that the irradiation entering from the side of the CPC which is made of acrylic has not been considered. This irradiation could result in an increase in the power output measured in the experiments. Nevertheless, the method compares favorably to experiments results within the limits of experimental accuracy.

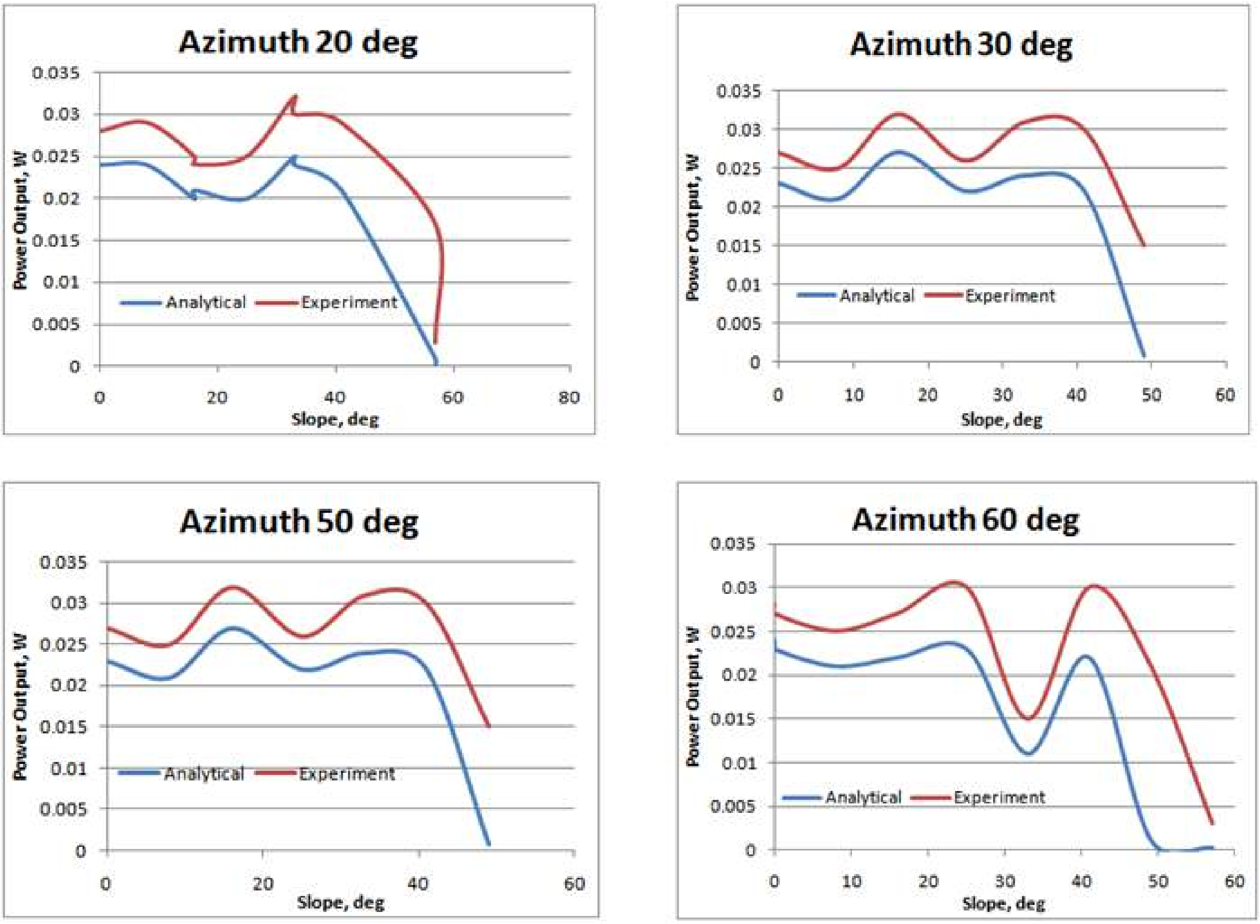

Fig. 6: Comparison of Experimental results with Analytical model results at different azimuths and different slopes

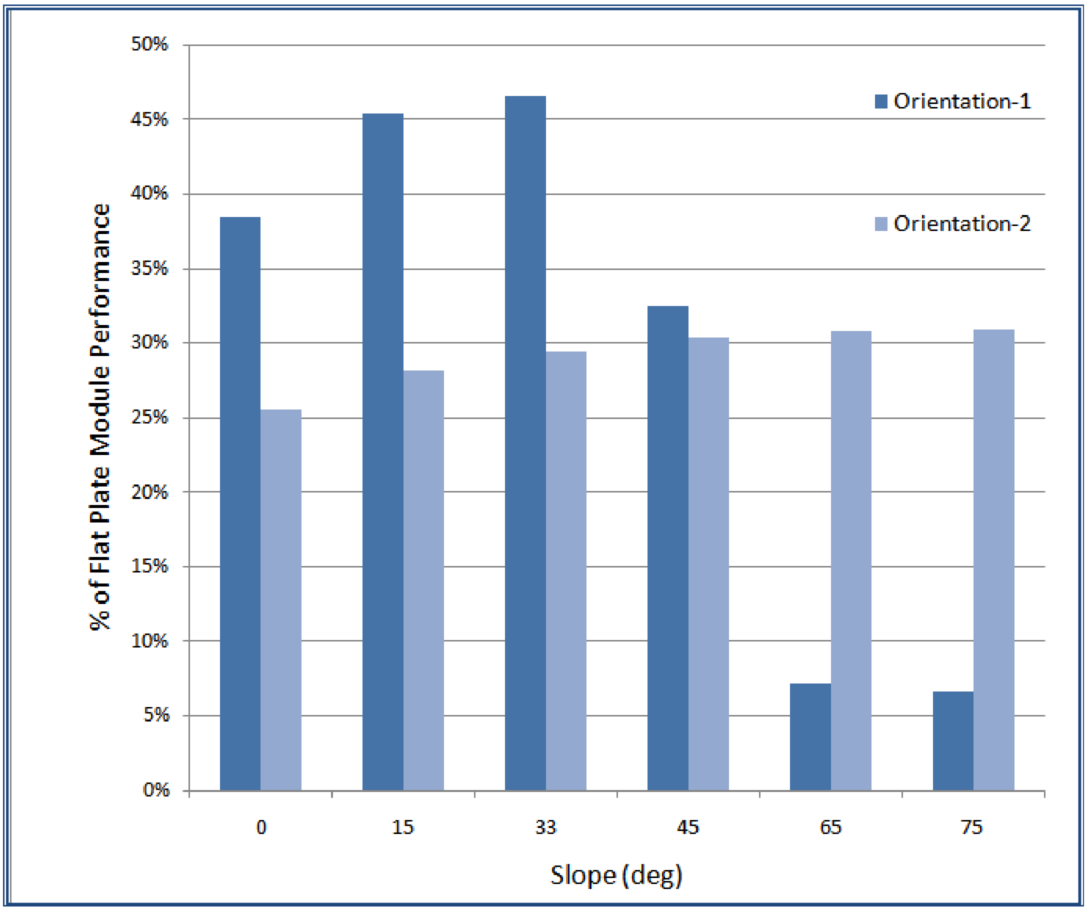

Fig. 7: Predicted Annual Performance of CPV expressed as a percentage of Annual Flat Plate Module Performance

5. ANNUAL MODEL

The methodology is now implemented for an entire year for the annual model. The Typical Meteorological Year Three (TMY3) hourly data from National Renewable Energy Laboratories, for Concord, New Hampshire was used for this calculation. The CPV is given a south facing azimuth, as this study is carried out in the northern hemisphere (it was also experimentally verified that this is the ideal collector azimuth). The power output of the CPV at each of the two orientations for different collector slopes is evaluated, as can be seen in Fig 7. The performance is expressed as a percentage of the power output of a flat module tilted at a similar slope and facing south. The area of the flat plate module is equal to the aperture area of the CPV.

6. RESULTS

The annual model as shown in Fig 7 demonstrates that optimal performance is attained at low roof slopes while the CPV is aligned “east-west” in orientation-1. However, at higher collector slopes, CPV aligned “north-south” in Orientation-2 offers better performance.

7. RECOMMENDATIONS

In future, a more detailed model could be developed incorporating the irradiation that enters through the side of the CPC. A module could be built and tested instead of a cell, for less discretization error. Finally, more tests could be conducted on the orientation-2. Field tests for prolonged periods of time could provide useful data on temperature Effects and point out any errors in the analytic model which have not surfaced in the laboratory tests. Also, the transmittance through the plastic could be modeled in more detail, as a function of incident angle.

8. NOMENCLATURE

$\vec{N}$ - Vector normal to the base (PV) of the CPC

$\vec{S}$ - Vector representing the Sun

$\vec{P}$ - Vector in the plane of the PV (at the base of the CPC) and the horizontal plane.

$\overrightarrow{Sproj}$ - Vector representing the projection of the Sun vector onto the plane of the normal to the collector (which is the plane of interest)

I_{cpv} - The total incident irradiation reaching inside the CPV

I_{beam} - Beam incident irradiation entering the CPV this is not equal to the entire beam incident irradiation, a correction is made in the form of the incidence angle..

I_D - Diffuse radiation entering the CPV

ρ_g - Ground reflectance

ΔTc - Increase in the temperature of CPV, this is calibrated from the ambient temperature, when not measured directly

$\Delta P\%$ - Temperature effect on power produced by the PV [%/℃]. In this study, 0.38%/oC has been used.

A_{lens} - Aperture area of the CPV, which is the area of the lens

η - Efficiency of the CPV

τ - Transmittance of the lens material. In this study, acrylic lens with a transmittance of 0.92 is used

θp1 - Solar profile angle on the CPV in Orientation-1 (“east-west”)

θp2 - Solar profile angle on the CPV in Orientation-2 (“north-south”) the angle between the normal $\vec{N}$ to the PV and the projection of the sun $\overrightarrow{Sproj}$ onto a plane defined by $\vec{N}$ and $\vec{P}$

i_N - Solar incidence angle on the plane normal to the collector plane

β - Collector slope

i - Solar incidence angle

a_w - Collector azimuth

aa_{cpc} - Acceptance angle of the CPC

CR - Concentration Ratio of the CPC (2.9 in this study)

z - Solar zenith angle

α - Solar altitude angle

a_s - Solar azimuth angle

All angles have been considered in radians.

9. ACKNOWLEDGEMENTS

The authors gratefully acknowledge the contribution of instrument to Chigbo Mgbemene.

10. REFERENCES

(1) John Duffy, Solar Systems Engineering & Solar Fundamentals Online Courses, University of Massachusetts, Lowell, 2008

(2) NSRDB, TMY3 records for Concord, NH http://rredc.nrel.gov/solar/old_data/nsrdb/1991-2005/tmy3/by_state_and_city.html

(3) John A. Duffie, William A. Beckman, Solar Engineering of Thermal Processes, Wiley, 2006

(4) Stuart R. Wenham, Martin A. Green, Muriel E. Watt, Richard Corkish, Applied Photovoltaics, 2nd edition, Earthscan, 2007

(5) Roland Winston, Juan C. Miñano, W. T. Welford, Pablo Benítez with contributions by with contributions by Narkis Shatz and John C. Bortz, Nonimaging Optics, Elsevier Academic Press, 2005

(6) D. Yogi Goswami, Frank Kreith, Jan F. Kreider Principles of Solar Engineering, 2nd edition, Taylor and Francis, 2000

(7) Sneha Sriwastava, University of Massachusetts, Lowell, MS Project, Annual Performance of a Compound Parabolic Concentrator Integrated Photovoltaics, 2009